Statistical Analysis of the Global Energy Confinement Time τ_E in Ohmic Discharges in the ASDEX Tokamak

E.E. Simmet

IPPIII/205

Sept 1995

MAX-PLANCK-INSTITUT FÜR PLASMAPHYSIK

85748 GARCHING BEI MÜNCHEN

MAX-PLANCK-INSTITUT FÜR PLASMAPHYSIK

GARCHING BEI MÜNCHEN

Statistical Analysis of the Global Energy Confinement Time τ_E in Ohmic Discharges in the ASDEX Tokamak

E.E. Simmet

Max–Planck–Institut für Plasmaphysik,
EURATOM–IPP Association,
Garching/München, Germany

Die nachstehende Arbeit wurde im Rahmen des Vertrages zwischen dem Max-Planck-Institut für Plasmaphysik und der Europäischen Atomgemeinschaft über die Zusammenarbeit auf dem Gebiete der Plasmaphysik durchgeführt.

Statistical Analysis of the Global Energy Confinement Time τ_E in Ohmic Discharges in the ASDEX Tokamak

E.E. SIMMET, ASDEX TEAM
Max–Planck–Institut für Plasmaphysik,
EURATOM–IPP Association,
Garching/München, Germany

Abstract: In ohmic discharges in all tokamaks at low plasma densities the global energy confinement time τ_E increases almost linearly with the density (LOC, Linear Ohmic Confinement). In tokamaks with sufficiently large dimensions τ_E saturates at a critical density (ASDEX: $\overline{n_e} \approx 3 \times 10^{19}\ m^{-3}$) and is nearly constant at higher densities (SOC, Saturated Ohmic Confinment). In the same density region some experiments report a further confinement regime for deuterium discharges in which τ_E exceeds the saturated value and is further increased (IOC, Improved Ohmic Confinement). There the global energy confinement time roughly behaves as in the LOC regime. For both the LOC and the SOC regimes an isotope effect, i.e. the dependence of τ_E on the ion mass, is reported as an additional aspect of the ohmic energy confinement.

A statistical analysis is performed to identify the parameters which are responsible for the properties of the energy confinement in these discharges in ASDEX. Contrary to earlier reports on confinement time scalings in ASDEX OH, only discharges with a full experimental description of kinetic electron and ion parameters, i.e. profiles of densities, temperatures and Z_{eff}, are used to evaluate the energy contents of both species. By means of statistics it is shown that the characteristics of τ_E are mainly caused by the behaviour of the electron energy flux and the ohmic input power. The ion energy flux, however, does not play a significant role. Furthermore, the IOC regime is explained as a continuation of the low–density LOC regime. Both effects, the isotope effect and the density dependence of τ_E, are caused by the features of the electron energy transport.

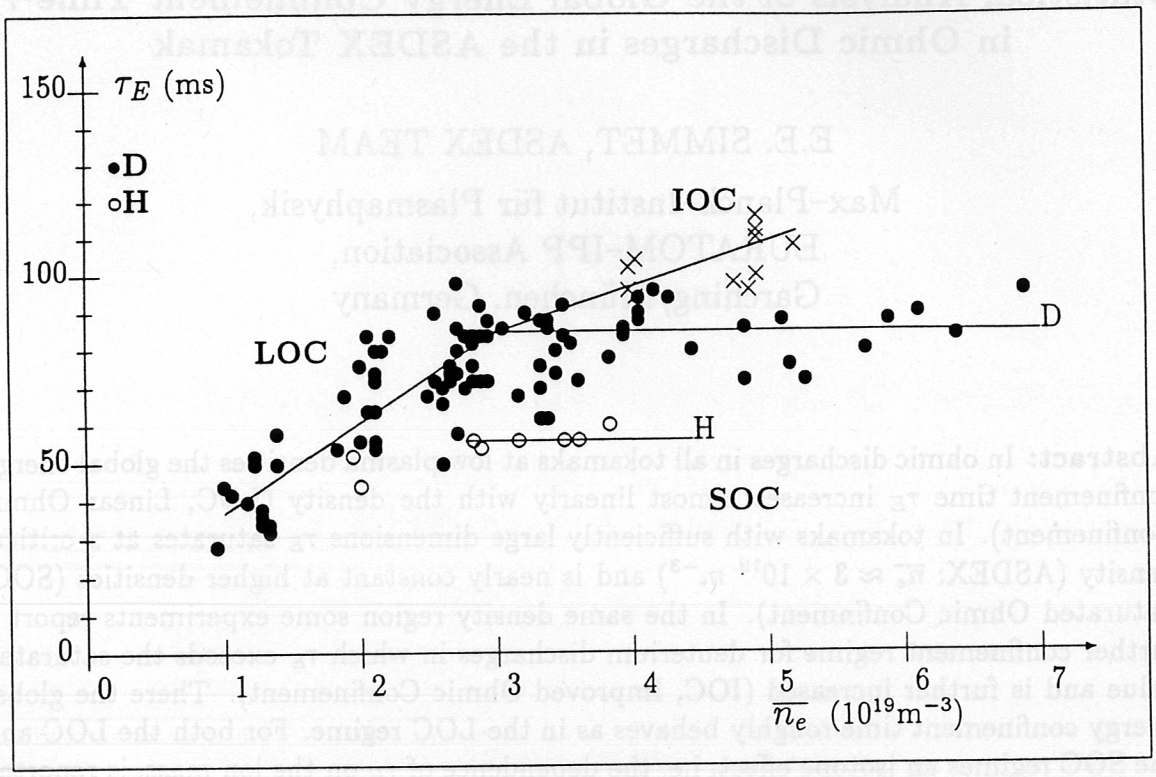

Figure 1: Energy confinement time in ohmic discharges in ASDEX. Due to the different dependences on the line–averaged density three confinement regimes are defined: LOC (low density, linear τ_E), SOC (high density, saturation) and IOC (high density, again linear).

1 Introduction

The ohmic energy confinement time τ_E of stationary discharges is defined here by the fraction of the total plasma energy, i.e. the energy of the electrons, E_e, and the energy of the plasma ions, E_i, and the ohmic input power P_{OH}:

$$\tau_E = \frac{E_e + E_i}{P_{OH}} \quad . \tag{1}$$

Although τ_E can be determined experimentally as a global parameter, it cannot provide significant information about the local mechanisms of the energy transport. Nevertheless, an additional analysis of the global energies and the ohmic power shows whether the dependences of the electron or the ion energy dominate the behaviour of τ_E. This affords the possibility of concentrating future work on the local transport properties of the most important loss channel in the power balance, electron or ion energy transport.

Ohmic discharges where only the electrons are heated externally can be seen as the simplest type of tokamak plasmas. Hence, with these discharges the characteristics of

τ_E and a knowledge of the most influential parameters are of fundamental importance for a general understanding of the energy confinement in tokamak plasmas. The work here is restricted to this ohmic case.

The behaviour of the global energy confinement time of ohmic discharges — especially its dependence on the line–averaged plasma density $\overline{n_e}$ — causes a natural classification of the whole ohmic scenario into three confinement regimes. This situation is presented for ohmic discharges in ASDEX in Fig. 1, where τ_E is plotted as a function of $\overline{n_e}$. At low plasma densities τ_E increases almost linearly with the density (LOC, Linear Ohmic Confinement). This confinement regime is observed in all tokamak experiments. When a critical density is reached, τ_E saturates and keeps constant when the density is further increased (SOC, Saturated Ohmic Confinement). Unlike the LOC regime, the SOC regime could not be found in small tokamaks, e.g. Alcator A [1] whereas in Pulsator [2] the saturation was observed at the upper densities, where operation was still possible. In experiments with sizes comparable to or even larger than ASDEX (R = 165 cm, a = 40 cm) the SOC is clearly identified and established within a large density range. In ASDEX, for instance, the critical density at which the LOC–SOC transition occurs is about 3×10^{19} m^{-3}, while the upper density for controllable operations is 2–3 times as high.

In both confinement regimes experiments with hydrogen and deuterium show different values of τ_E. In ASDEX the saturated values are 50–60 ms for hydrogen and 80–90 ms for deuterium (see Fig. 1). This isotope effect with τ_E approximately proportional to $\sqrt{A_i}$, with the mass number A_i (1:H, 2:D), is reported for the LOC and SOC regimes in almost all tokamaks, where experiments with both isotopes have been performed, e.g. JET [3] and FT [4].

In addition to LOC and SOC, a further confinement regime with improved τ_E was found in ASDEX [5]. For deuterium discharges with strongly reduced gas puffing rates at plasma densities comparable to the SOC regime the energy confinement time exceeds the saturated values. In this regime (IOC, Improved Ohmic Confinement) τ_E roughly behaves as in the LOC regime: it increases with increasing plasma density and values of around 130–150 ms are reached at the highest densities in ASDEX [5].

A lot of models have been discussed to explain the three different confinement regimes as results of different transport mechanisms. The LOC regime is connected with discharges where the electron heat transport dominates the total energy transport [6]. The electron heat conductivity is found to scale inversely to the plasma density, $\chi_e \sim 1/n_e^{0.8}$ (Coppi–Mazzucato–Gruber scaling) [2]. This may be due to, for example, drift wave turbulence, which would also result in an almost linear dependence of τ_E on the plasma density [7]. The ions are expected to play only a minor role in this regime.

To explain the LOC–SOC transition two situations have been discussed. For small tokamaks such as Pulsator or ISX–A the ion energy transport is found to be neoclassical [2, 8]. There an increase of the plasma density leads to increased ion energy losses and — following the Coppi–Mazzucato–Gruber scaling — to decreased electron energy losses. The saturation then occurs at a critical density where the ion energy losses become the dominating part in the power balance. A degradation of τ_E at higher densities is observed

which is also due to the dominating neoclassical ion losses [8, 9]. This behaviour is in contrast to that in larger tokamaks such as ASDEX, where τ_E is almost constant above the transition density.

Modifications of both the ion and electron energy transport have therefore been proposed to explain the saturation in large–scale tokamaks. A first model connects the saturation with some anomalous ion energy transport mechanisms which should dominate the total energy transport in SOC discharges, while they should be of less importance in LOC according to the upper model. The most popular candidates are the ion temperature gradient driven modes [10, 11]. In a second model [6] the electron behaviour is held responsible for the saturation. The saturation should occur at a plasma density where the electron heat conductivity itself significantly changes and does not further decrease with rising density.

A possible explanation for the IOC regime is given in [12]: While an anomalous ion energy transport is proposed there for SOC discharges, it is expected to be suppressed in IOC discharges. In [6] another explanation is found: Similarly to the behaviour in LOC discharges, non–saturated electron heat conduction causes τ_E to rise in IOC.

In this paper it is shown that in all three regimes the ohmic confinement time is mainly dominated by the dependences on the electron energy flux and the ohmic power. This holds for both the density scaling and the isotope effect. It is further shown that the ion energy and hence the underlying ion energy transport only play a minor role in all three confinement regimes in ASDEX. The basic mechanisms governing the behaviour of τ_E in all ohmic regimes are the electron heat transport and the quality of the coupling of the ohmic power to the electrons, which are both different at least between LOC and SOC or SOC and IOC.

This paper is organized as follows: Section (2) contains scaling laws of τ_E for the different confinement regimes in ASDEX. In the sections (3) and (4) the properties of the ohmic heating power and the energies of the electrons and ions are discussed. These results are used in section (5) to reconstruct the energy confinement time and show the importance of the electron energy transport and the ohmic heating characteristics.

2 Statistical Analysis of τ_E

In order to evaluate the ohmic energy confinement time as defined in Eq. (1), the energies E_e and E_i were both calculated from local data, i.e. radial profiles of density and temperature. Only discharges with steady–state phases of at least a few hundred milliseconds were analyzed.

The electron density and temperature are measured with a 16–channel Thomson scattering diagnostic [13], while the radial profile of the ion temperature $T_i(r)$ is determined from a single–chord CX diagnostic [14, 15] during series of identical discharges. The profile of the effective ion charge $Z_{eff}(r)$ is obtained from a multichord measurement of bremsstrahlung [16]. As direct measurement of the radial profile of the ion density $n_i(r)$ is not possible in ASDEX, this profile is calculated from the electron density and

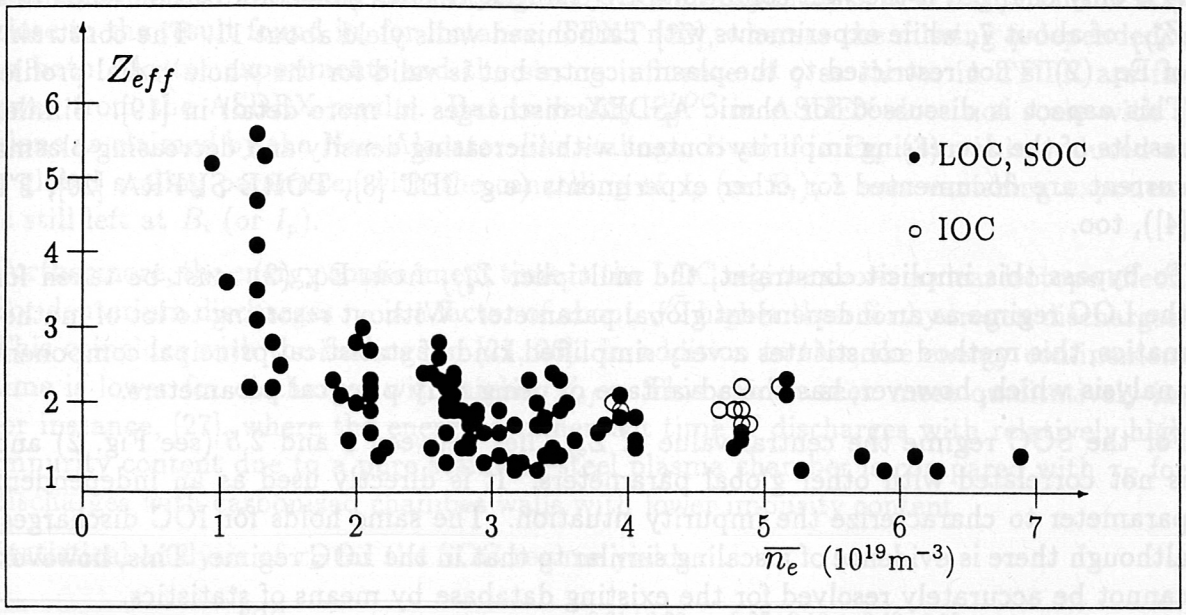

Figure 2: In the linear ohmic regime Z_{eff} scales almost inversely to the plasma density. In both of the other regimes no significant tendency is observed.

$Z_{eff}(r)$. Under normal experimental conditions in ASDEX the impurity ions are a mix of carbon and oxygen and an averaged impurity charge of 7 is fixed [17]. The ion density is then calculated with $n_i(r) = n_e(r) \times (7 - Z_{eff}(r))/6$.

Finally, the ohmic power is determined from the experimentally measured loop voltage U_l and the plasma current I_p.

For the statistical analysis of τ_E only externally controlled global parameters are used. These are the line–averaged electron density $\overline{n_e}$ with a range of 1.0 to 7.1×10^{19} m^{-3} (where the roll–over density in ASDEX is 3×10^{19} m^{-3}), the total plasma current I_p (220–460 kA), the toroidal magnetic field B_t (1.7–2.8 T), the atomic mass number A_i (1: hydrogen, 2: deuterium) and the effective plasma charge Z_{eff} (1.1–6.0 in the centre). Here it must be taken into account that Z_{eff} can in principle be externally controlled by controlling or changing the wall conditions. In the ASDEX tokamak the techniques possible were carbonization and boronization [18].

The first few of the parameters given above are independent variables. In contrast to this, Z_{eff} depends on the density and current in the LOC regime. Linear regression analysis demonstrate that

$$Z_{eff}^{LOC}(0) = Z_{eff}^{*}\ \overline{n_e}^{\,-0.88} I_p^{0.51}\ , \qquad (2)$$

where the factor Z_{eff}^{*} does not depend on $\overline{n_e}$ and I_p. Here and in the following scaling laws $\overline{n_e}$ is given in units of 10^{19} m^{-3} and I_p in units of MA. To illustrate the decreasing effective charge with increasing plasma density the central value $Z_{eff}(0)$ is plotted versus $\overline{n_e}$ in Fig. 2. Z_{eff}^{*} in Eq. (2) directly reflects the impurity composition at the walls and

it is only changed if the wall conditions are changed. In ASDEX boronization leads to a Z^*_{eff} of about 7, while experiments with carbonized walls yield about 11. The constraint of Eq. (2) is not restricted to the plasma centre but is valid for the whole radial profile. This aspect is discussed for ohmic ASDEX discharges in more detail in [19]. Similar results of the decreasing impurity content with increasing density and decreasing plasma current are documented for other experiments (e.g. JET [3], TORE SUPRA [20], FT [4]), too.

To bypass this implicit constraint, the multiplier Z^*_{eff} from Eq. (2) must be taken for the LOC regime as an independent global parameter. Without resorting to lot of mathematics, this method constitutes a very simplified kind of statistical principal component analysis which, however, has the advantage of using only physical parameters.

For the SOC regime the central value of Z_{eff} lies between 1 and 2.5 (see Fig. 2) and is not correlated with other global parameters. It is directly used as an independent parameter to characterize the impurity situation. The same holds for IOC discharges, although there is evidence of a scaling similar to that in the LOC regime. This, however, cannot be accurately resolved for the existing database by means of statistics.

With the global parameters listed above, τ_E behaves as

$$\begin{aligned} \tau_E^{LOC} &= (17 \pm 2) ms \times \overline{n_e}^{0.86 \pm 0.07} I_p^{-0.66 \pm 0.09} B_t^{0.31 \pm 0.20} \\ &\times A_i^{0.43 \pm 0.10} Z^*_{eff}{}^{-0.30 \pm 0.10} \end{aligned} \tag{3}$$

for discharges of the LOC regime in ASDEX.

In earlier work on ohmic ASDEX discharges another scaling law is discussed [21], which is repeated in, for instance, [22]. There, however, a density scaling proportional to $\overline{n_e}^{0.39}$ is calculated for LOC discharges. For two reasons this low exponent is wrong. First, from a statistical point of view, in the scaling laws of [21] Z_{eff} is used like an independent variable which does not depend on density and current. Therefore, a large fraction of the real density variation of τ_E is hidden in the Z_{eff}–dependence and the resulting exponent calculated at $\overline{n_e}$ is too small. Considering Fig. 1, it is obvious that $\overline{n_e}^{0.39}$ would give confinement times which are about 40% too low in relation to the experimental values. A further consequence is that scaling laws for the LOC regime in ASDEX from [21, 22] are not correct if the exponent at Z_{eff} does not vanish there.

Despite the fact that a scaling with minor radius a and major radius R is not possible due to the small variations of both parameters in ASDEX, the scaling law (3) is close to the Neo–Alcator scaling $\tau_E^{Neo-A} \sim \overline{n_e} \times q^{1/2}$ [1] and to modifications with $\tau_E \sim \overline{n_e} \times q_a^{\alpha}$ (e.g. $\alpha = 0$ for Alcator A, Alcator C [1], $\alpha = 1/2$ for TEXT [23], $\alpha = 3/4$ for Doublet III [24], $\alpha = 1$ for TFTR [25]).

The density dependence in ASDEX LOC is somewhat weaker than predicted by the Neo–Alcator scaling. The exponent 0.86, however, is a statistically significant result for the ASDEX–LOC and it is very unlikely that the energy confinement time τ_E^{LOC} (Eq. (3)) behaves exactly like the Neo–Alacator scaling.

The q–dependence as reported for the experiments listed above has its counterpart in ASDEX LOC, too. Linking the plasma current and the toroidal field to a common q

scaling simply by averaging their exponents yields an exponent of 0.48 for q. This is very close to the result found in, for instance, TEXT [23], whereas the missing q-dependence in both Alcator experiments and the strong influence of q as shown in TFTR are far away from the ASDEX results. But in reality τ_E^{LOC} in ASDEX does not scale with q alone as claimed by the Neo–Alacator–like scalings. Even if in Eq. (3) q is introduced as a global scaling parameter with the cancelling of I_p (or B_t), a non–vanishing exponent is still left at B_t (or I_p).

Furthermore, the energy confinement time in the LOC regime shows a clear isotope effect. For deuterium discharges τ_E is a factor of about $\sqrt{2}$ higher than for hydrogen discharges. This coincides with the findings in [21, 26]. In addition to this, the energy confinement time is lower for discharges with higher Z_{eff}. This can be seen more qualitatively in, for instance, [27], where the energy confinement time of discharges with relatively high impurity content due to a pure stainless–steel plasma chamber is compared with τ_E for discharges with carbonized chamber walls with lower impurity content.

Statistical analysis of τ_E for the SOC regime yields

$$\begin{aligned} \tau_E^{SOC} &= (23 \pm 3) ms \times \overline{n_e}^{0.21 \pm 0.09} I_p^{-0.27 \pm 0.12} B_t^{0.40 \pm 0.13} \\ &\times A_i^{0.48 \pm 0.10} Z_{eff}^{-0.10 \pm 0.10} . \end{aligned} \tag{4}$$

As suggested by Fig. 1, only small variations with the density occur for the SOC regime. The current scaling is weaker than in the LOC regime, although in both regimes τ_E increases with decreasing current. In contrast, the dependence on B_t is almost identical for the two scaling laws. An alternative scaling law where q is used as a regression variable instead of the current and the magnetic field therefore yields a scaling close to $q^{1/3}$ which is clearly weaker than for LOC discharges. A comparison of the exponents at A_i of the two regimes shows that the transition from LOC to SOC does not influence the isotope effect at all. Finally, it must be concluded that the influence of impurities is slightly different in LOC and SOC discharges.

The IOC scaling roughly behaves as the LOC scaling with regard to the density and the wall conditions (see the Z_{eff}^*–dependence in Eq. (3) and the Z_{eff}-dependence in Eq. (5)), although the density scaling is somewhat weaker in the IOC regime. Owing to the poor variation of the plasma current and the toroidal magnetic field in the sub–database of IOC discharges and to the impossibility of reaching this regime with pure hydrogen, from the point of view of statistics no statement about these global values is allowed. For this reason they are ignored in all scaling laws relating to IOC. The scaling law for τ_E in the IOC regime therefore reads

$$\tau_E^{IOC} = (47 \pm 5) ms \times \overline{n_e}^{0.62 \pm 0.19} Z_{eff}^{-0.35 \pm 0.16} . \tag{5}$$

3 The Ohmic Power

To explain the dependences of τ_E in the different regimes, first the role of the ohmic power appearing in the definition given in Eq. (1) must be explored.

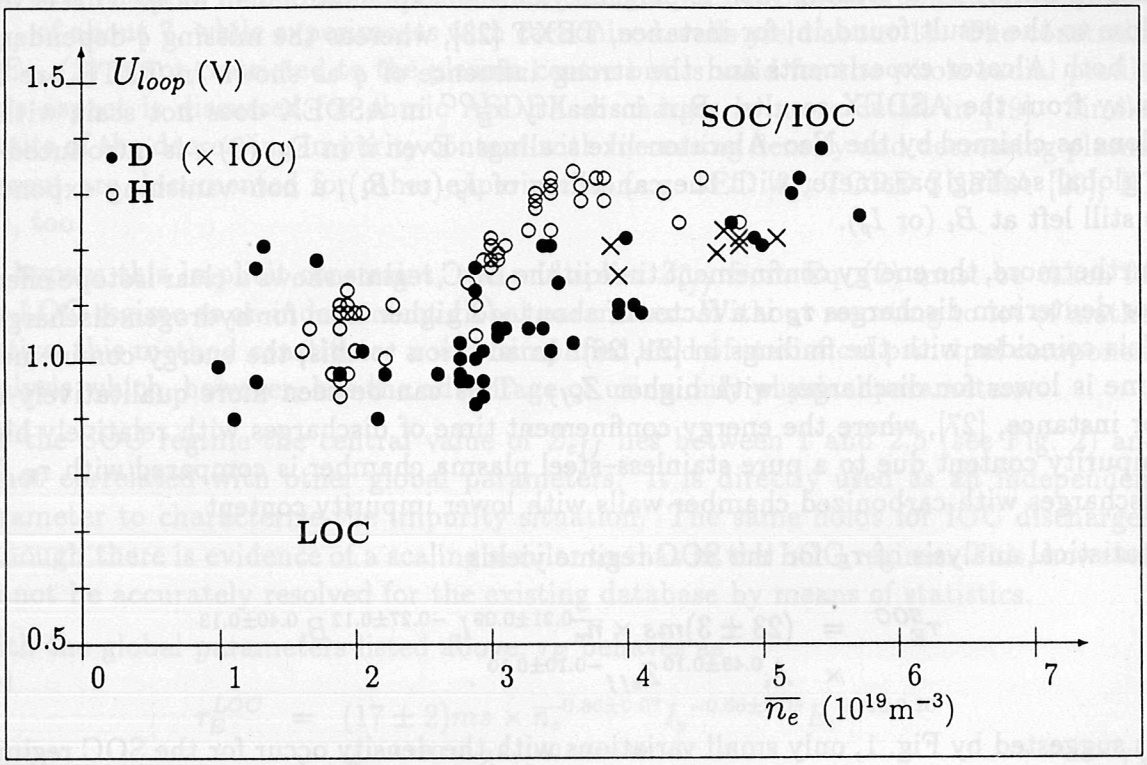

Figure 3: For LOC and IOC discharges the loop voltage U_L does not depend on the plasma density. In the SOC regime it slightly increases with the plasma density. In the IOC regime U_L exceeds the SOC values due to the higher impurity content.

Applying the same regression models to the ohmic power as used above for τ_E yields

$$P_{OH}^{LOC} = 1.15MW \times \overline{n_e}^{0.00\pm0.06} I_p^{1.45\pm0.15} B_t^{-0.17\pm0.19} \times A_i^{-0.16\pm0.05} Z_{eff}^{*\,0.31\pm0.08}, \quad (6)$$

$$P_{OH}^{SOC} = 1.45MW \times \overline{n_e}^{0.31\pm0.06} I_p^{1.15\pm0.08} B_t^{-0.41\pm0.09} \times A_i^{-0.17\pm0.04} Z_{eff}^{0.00\pm0.05}, \quad (7)$$

$$P_{OH}^{IOC} = 0.28MW \times \overline{n_e}^{0.00\pm0.08} Z_{eff}^{0.24\pm0.07}, \quad (8)$$

where for the IOC regime the influence of I_p, B_t and A_i is unknown.

In general, P_{OH} is derived from the product of the loop voltage U_l and the plasma current I_p. Hence, dividing the upper scaling laws (6–8) by the current directly leads to expressions for the loop voltage.

As can be seen, the reason for the dependence of the ohmic power on, for instance, the density (SOC) or the isotope mass (LOC, SOC) is a consequence of the behaviour of the loop voltage, or in a more direct manner, of the toroidal electric field induced by the ohmic transformer. To illustrate the density dependence of U_l, Fig. 3 shows the loop voltage as a function of $\overline{n_e}$. For the LOC and IOC regimes no variation with the density

is observed, while in the SOC regime a weak increase with increasing $\overline{n_e}$ is deduced. If one considers the variation of the ohmic power with the impurity parameter, the IOC scaling looks like a continuation of the LOC scaling due to exponents which are both close to 0.3. Here again the SOC discharges obviously show a different behaviour. In this regime the scaling (7) is absolutely independent of any influence of Z_{eff}. Apart from the same signs of the exponents of I_p and B_t in the LOC and SOC scalings, no common conclusion can be made for the two regimes as far as one of these parameters is concerned. While the ohmic power strongly depends on I_p in LOC — with an exponent 1.45, which is clearly far from unity — it scales almost proportionally to the current with an exponent of 1.15 in SOC. The scaling with B_t is in contrast to the current scaling in the opposite direction. Here the LOC scaling possesses only a small exponent of -0.17, while in SOC an exponent twice as high (-0.41) is deduced. These differences in I_p and B_t cannot be explained by assuming an additional q–dependence in SOC.

Another situation occurs if the isotope mass is varied. In both regimes, LOC and SOC, P_{OH} behaves in the same way. Going from pure hydrogen to pure deuterium discharges, the ohmic power needed to establish the same current and field configurations for both isotopes decreases as $A_i^{1/6}$. Hence, producing the same plasma current at the same magnetic field and plasma density requires about 10% more ohmic heating power in hydrogen than in deuterium. On the other hand, coupling the same power to these discharges results in a lower current in hydrogen, which results in a substantially changed poloidal magnetic field configuration. For this reason the isotope effect of the energy confinement time τ_E in both the LOC and SOC regimes at fixed magnetic configuration — by fixing the safety factor q_a at the plasma edge — and at constant ohmic power can be calculated to be close to 0.2 to 0.3 by principal component analysis instead of the 0.5 obtained by using the induced current as an independent parameter.

Simulations of the radial profile of the induced current density [19] show that in all three regimes the ohmic current is well described by the neoclassical formula for the resistivity [28]. Hence, the differing scaling laws for P_{OH}, especially the density scaling and the isotope effect, mainly reflect the different behaviour of the electron temperature and impurity content in these regimes. There is no hint that the mechanism of inducing the ohmic current changes during a transition from LOC to SOC or from SOC to IOC.

Taking into account the inverse scaling of τ_E with I_p and the higher than linear scaling of the ohmic power with the current in the LOC and SOC regimes, one can presume a kind of power degradation as proposed by Bartiromo [29] for ohmic tokamak discharges. In [29] the ohmic confinement time is given by

$$\tau_E^{OH} \sim \overline{n_e}^{0.55} I_p^{0.75} B_t^{0.2} A_i^{0.3} P_{OH}^{-0.75} . \quad (9)$$

This scaling law is deduced from data of several tokamaks including both LOC and SOC discharges. Z_{eff} and q_a dependences are neglected there. Rearranging the scaling laws, Eq. (3) for LOC and Eq. (4) for SOC yields

$$\tau_E^{LOC} \sim \tau_E^{OH} \times \overline{n_e}^{0.3} I_p^{-0.3} , \quad (10)$$

$$\tau_E^{SOC} \sim \tau_E^{OH} \times \overline{n_e}^{-0.1} I_p^{-0.25} q_a^{-0.1} . \quad (11)$$

As τ_E^{OH} is based upon data of both regimes, the density exponent 0.55 must be seen as an average which has to lie between the linear and saturated cases. This simply explains the discrepancies of the density scalings between τ_E^{LOC} and τ_E^{OH} ($\overline{n_e}^{0.3}$) and between τ_E^{SOC} and τ_E^{OH} ($\overline{n_e}^{-0.1}$).

The differences in the exponents of the current can be explained by the fact that tokamaks with larger major and minor radii R and a, respectively, operate at higher currents than smaller tokamaks. In regression analyses, where both radii are included in addition to the parameters given above, the resulting exponents at R, a and I_p are coupled. Hence, as such an analysis has been performed in [29], there can be systematic deviations — without changing the accuracy of the results — from the current dependence as found for the ASDEX database used here. This can be observed by looking at Eq. (10,11), where the two exponents of I_p are almost identical and close to -0.3.

Nevertheless, the scaling laws for the energy confinement time of ohmic ASDEX discharges compare satisfactorily with data from several tokamaks as given by Eq. (9). In addition, the ASDEX data agree well with a power degradation proportional to $P_{OH}^{-0.75}$ as given in [29].

A further question which arises when the ohmic power input is discussed concerns the fractions of P_{OH} which are transported via the electrons and the ions. Without discussing the full spectrum of the local energy transport of both species [19], this question can be answered by taking a look at the power transfer Q_{ei} from the electrons to the ions due to collisions. As Q_{ei} is proportional to the expression $n_e^2(T_e - T_i)/T_e^{3/2}$, it is available from direct measurements. The same holds for the integrated power $P_{ei}(r)$, which is the total power transferred inside a flux surface with radius r.

It must be taken into account that in ohmic discharges the ion temperature is lower than the electron temperature only in the inner region and that $T_i(r)$ exceeds $T_e(r)$ in the outer part of the plasma. At a radius close to $r{=}a/2$ to $3a/4$ the two temperatures become equal. Hence, P_{ei} taken at these radii approximately gives the upper limit of the total transferred power and is representative of the highest transferred power.

At $a/2$, P_{ei} is as small as 10 kW at the lowest densities, while at $3a/4$ 20–30 kW is transferred to the ions [19]. With increasing plasma density, P_{ei} increases, too. At the density where the transition from LOC to SOC occurs, $P_{ei}(a/2)$ reaches about 20–40 kW and $P_{ei}(3a/4)$ reaches 30–70 kW. A linear dependence of P_{ei} on $\overline{n_e}$ in LOC is clearly identified. Although, due to the large error of P_{ei} at high plasma densities, the statistical variations are enlarged, this linear dependence is consistent with the high-density regimes, too.

A comparison of P_{ei} with the ohmic input power shows that the energy losses due to the ion energy transport play only a minor role for the total energy losses. With the discharges of our database, the total ohmic power is 300–400 kW in all three confinement regimes. The power lost via the ion energy transport is restricted, however, by P_{ei}. For LOC discharges, this is at most only one-third of P_{OH}. This is further explained by Fig. 4. This figure shows the ratio of P_{ei} to the ohmic power P_{OH} for the two radii. Here the ohmic powers $P_{OH}(a/2)$ and $P_{OH}(3a/4)$, respectively, are used. Variations at fixed densities come mainly from variations of the ohmic power. Nevertheless, Fig. 4 clearly

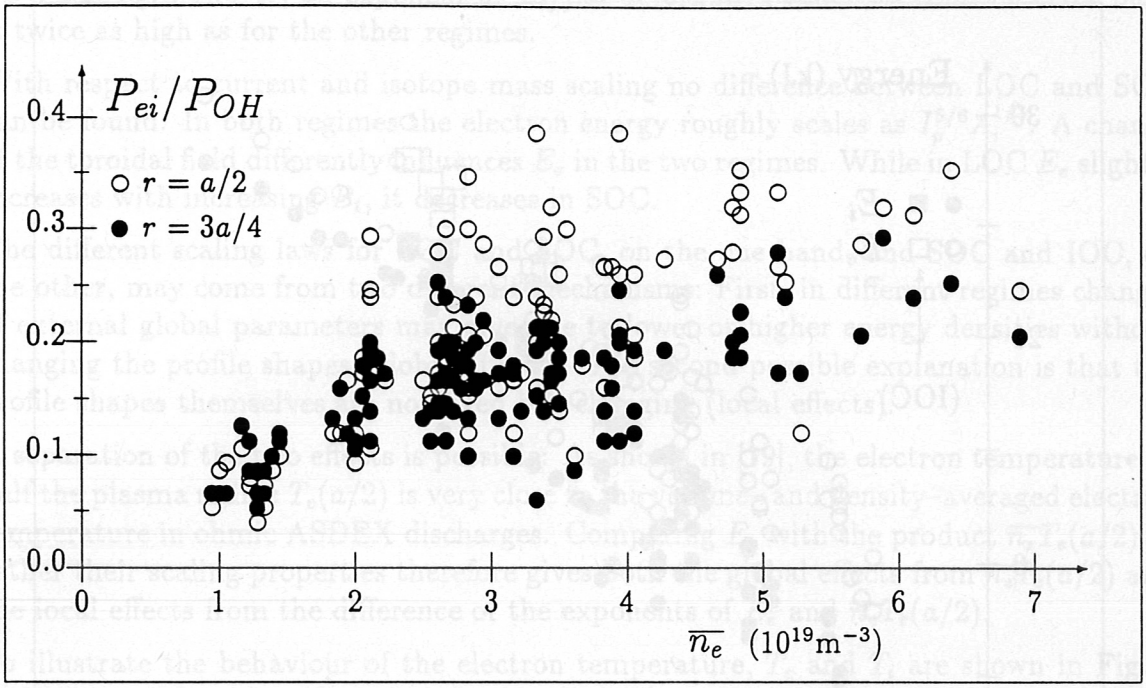

Figure 4: At low densities only 10 per cent of the total ohmic power is transferred to the ions. Although the ratio shown here is linearly dependent on the plasma density, even at the highest densities not more than about one–third is lost via the ion branch.

shows that at the lowest densities only one–tenth of the ohmic input is transferred from the electrons to the ions. This ratio P_{ei}/P_{OH} increases as the density. It reaches values of around one–third for $a/2$ but is less than 20% for $3a/4$ at the transition density. Because of the characteristics of P_{OH} in the SOC regime, as discussed above, P_{ei}/P_{OH} increases only slightly in this regime at both radii. For the whole high–density range this ratio is 10–35% at $a/2$ and about 10–30% at $3a/4$.

4 Scaling Laws for the Energies

As discussed above, the density dependence of τ_E in the LOC regime, for instance, is not the result of the scaling of the ohmic power. To explain this effect among other properties of the τ_E scalings and identify if they are caused by the electron or the ion behaviour, a regression analysis is necessary for both the electron energy and the ion energy.

The energies of both the electrons and the ions are illustrated in Fig. 5 for the whole density range. In low–density discharges the ion energy content is clearly below the electron energy content. This is primarily due to the large Z_{eff} values in this regime. Due to the steep decrease of Z_{eff} and better coupling of the two temperatures $T_e(r)$ and $T_i(r)$, the ion energy grows faster than the electron energy with increasing plasma

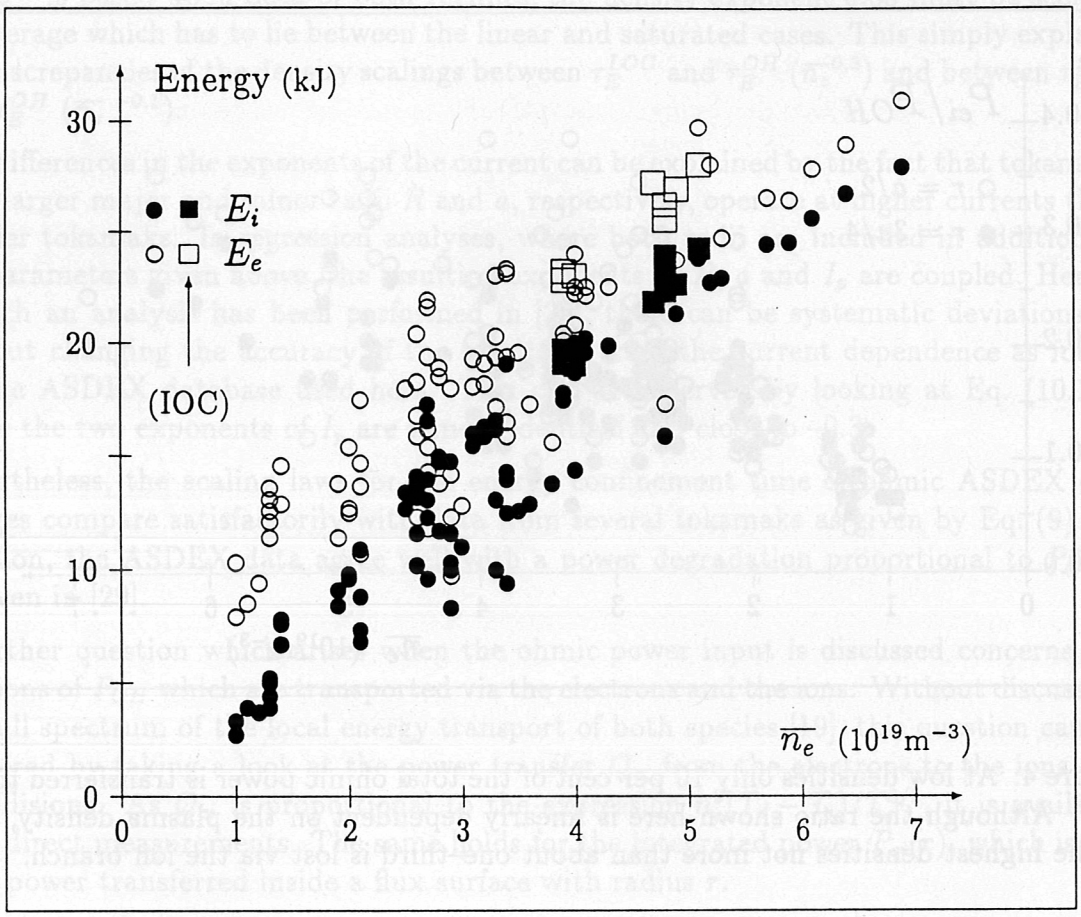

Figure 5: For all ohmic confinement regimes the electron energy grows as the plasma density, although the scaling is weaker than linear. Due to the behaviour of the impurities the ion energy increases faster in the LOC and IOC regimes than in the SOC regime.

density. Above the density where the LOC–SOC transition occurs the energies of the two species are almost identical.

Considering the statistical properties of the electron energy E_e in these regimes yields

$$\begin{aligned} E_e^{LOC} &= 10.6kJ \times \overline{n_e}^{0.61\pm0.03} I_p^{0.89\pm0.08} B_t^{+0.20\pm0.10} \\ &\times A_i^{0.33\pm0.06} {Z^*_{eff}}^{0.19\pm0.05}, \qquad (12) \\ E_e^{SOC} &= 20.3kJ \times \overline{n_e}^{0.48\pm0.13} I_p^{0.86\pm0.16} B_t^{-0.22\pm0.10} \\ &\times A_i^{0.26\pm0.06} Z_{eff}^{0.38\pm0.09}, \qquad (13) \\ E_e^{IOC} &= 10.4kJ \times \overline{n_e}^{0.55\pm0.23} Z_{eff}^{0.13\pm0.10}, \qquad (14) \end{aligned}$$

with almost the same density dependence in all three regimes. Within the error bars all exponents of $\overline{n_e}$ are close to 0.5–0.6, with a somewhat weaker dependence in the SOC regime than in the other two regimes. As deduced above for the ohmic power, again the IOC scaling ($\overline{n_e}$ and Z_{eff}) seems to reflect a continuation of the LOC regime. For the

SOC scaling, however, an exponent at Z_{eff} is determined which, within the error bars, is twice as high as for the other regimes.

With respect to current and isotope mass scaling no difference between LOC and SOC can be found. In both regimes the electron energy roughly scales as $I_p^{5/6} A_i^{1/3}$. A change of the toroidal field differently influences E_e in the two regimes. While in LOC E_e slightly increases with increasing B_t, it decreases in SOC.

The different scaling laws for LOC and SOC, on the one hand, and SOC and IOC, on the other, may come from two different mechanisms: First, in different regimes changes of external global parameters may give rise to lower or higher energy densities without changing the profile shapes (global effects). The second possible explanation is that the profile shapes themselves are not fixed but changing (local effects).

A separation of the two effects is possible: As shown in [19], the electron temperature at half the plasma radius $T_e(a/2)$ is very close to the volume– and density–averaged electron temperature in ohmic ASDEX discharges. Comparing E_e with the product $\overline{n_e} T_e(a/2)$ or rather their scaling properties therefore gives both the global effects from $\overline{n_e} T_e(a/2)$ and the local effects from the difference of the exponents of E_e and $\overline{n_e} T_e(a/2)$.

To illustrate the behaviour of the electron temperature, T_e and T_i are shown in Fig. 6 as functions of the density for two radii, 0 and 20 cm. In the plasma centre the electron temperature is well above the ion temperature in the low–density regime with a clear density dependence. As is generally known, increasing the plasma density yields almost identical electron and ion temperatures. In the SOC regime the ratio of $T_i(0)$ and $T_e(0)$ is close to 0.9–0.95, while in the IOC regime it is close to 1. Due to the improved energy confinement IOC discharges show higher temperatures than SOC discharges with equal density, current and magnetic field. This holds for all radii, as can be seen for, for instance, $r{=}a/2$ in the lower part of Fig. 6. In this confinement region around half the plasma radius the ion temperature normally exceeds the electron temperature in the high–density discharges discussed here, while in the LOC regime – due to the high central electron temperature – the two temperatures are equal at higher radii of around $2a/3$.

As can be seen from Fig. 7 the volume–averaged peaking factor of the electron temperature, Q_{T_e}, is 2–2.5. Because of the lower central values the ion temperature profile peaking is lower and yields factors of close to 2. In contrast to the temperature peaking, the density peaking factors for the two species Q_{n_e} and Q_{n_i} are comparable and lie within 1.5–2. Higher factors for the ion densities, as shown in the upper part of Fig. 7, are obtained for discharges where Z_{eff} increases strongly towards the plasma edge. For these discharges the peaking factor is not basically caused by the central values but by low ion density in the outer part of the plasma.

As shown in Tab. 1, in the three confinement regimes $T_e(a/2)$ scales as $\overline{n_e}^{\,-0.4}$ (LOC) and $\overline{n_e}^{\,-0.5}$ (SOC and IOC). These exponents are almost identical to the exponents of $E_e/\overline{n_e}$ in all three regimes. Hence, the density variation of the confinement time is only governed by the behaviour of the mean electron temperature and profile effects are not needed to explain it. The exponents of $T_e(a/2)$ for the plasma current are very close to 1 in both the LOC and SOC regimes. Hence, it can be concluded that the almost linear

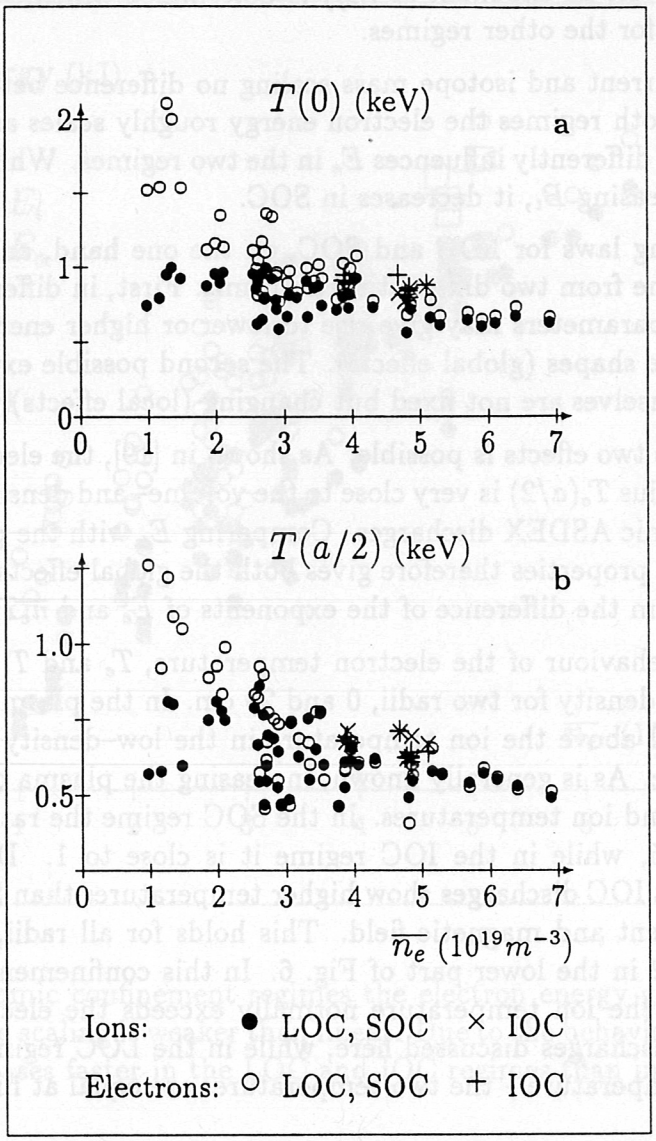

Figure 6: Temperatures in ohmic discharges for the plasma centre (a) and half the plasma radius (b).

increase of the temperature with the current causes the exponents of around 0.8–0.9 in the energy scaling laws in both regimes. No influence of profile effects can be seen here either.

It is different with the impact of the toroidal field on the scaling of the energy content. In the LOC regime $T_e(a/2)$ does not depend on B_t, while in the SOC regime it scales as $B_t^{-0.5}$. A comparison with the energy scaling laws shows that an additional exponent of around 0.2 must be caused by profile effects which are the same for LOC and SOC. An analysis of the electron density and temperature profiles indeed shows increased peaking of both profiles when the toroidal field is increased. This is mainly due to the fact that

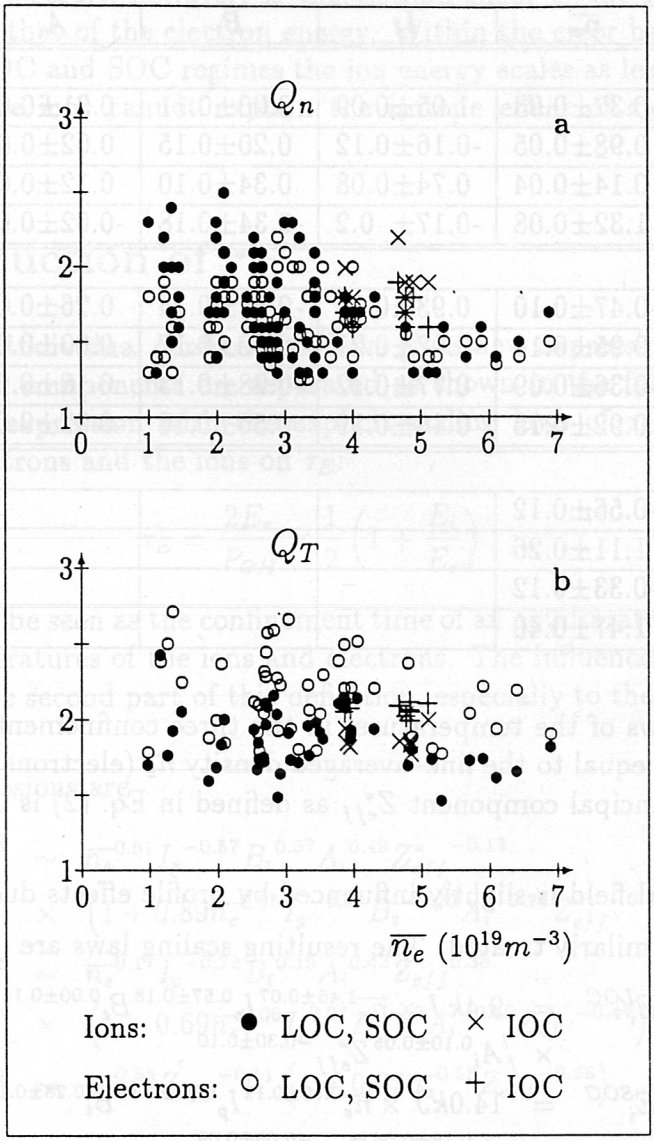

Figure 7: Peaking factors of densities (a) and temperatures (b) in ohmic discharges.

at higher toroidal fields the plasma volume where $q \leq 1$ is much more restricted to the plasma centre. Such a natural limitation of the sawtooth activity which tends to flatten the profiles inside the q=1 surface gives rise to peaking of the energy density profiles which is identical in the two regimes.

In contrast to the B_t exponents, the scaling of E_e with the mass number and Z_{eff} is totally explained by the behaviour of $T_e(a/2)$. The mean temperature depends on A_i with exponents 0.31 (LOC) and 0.26 (SOC) and on Z_{eff} with exponents 0.19 (LOC), 0.37 (SOC) and 0.20 (IOC), which are all almost identical to the exponents of Eqs. (12–14).

Summarizing these results shows that the scaling of the electron energy can be described by $E_e \sim \overline{n_e} T_e(a/2)$ very precisely in all three confinement regimes. Only the dependence

	$\overline{n_e}$	I_p	B_t	A_i	Z_{eff}
LOC					
$T_e(a/2)$	-0.37±0.03	1.05±0.09	0.00±0.11	0.31±0.06	0.19±0.05
$E_e/T_e(a/2)$	0.98±0.05	-0.16±0.12	0.20±0.15	0.02±0.08	0.00±0.07
$T_i(a/2)$	0.14±0.04	0.74±0.08	0.34±0.10	0.12±0.06	0.10±0.05
$E_i/T_i(a/2)$	1.32±0.08	-0.17± 0.2	-0.34±0.18	-0.02±0.08	-0.40±0.11
SOC					
$T_e(a/2)$	-0.47±0.10	0.93±0.13	-0.52±0.14	0.26±0.06	0.37±0.08
$E_e/T_e(a/2)$	0.95±0.16	-0.07±0.21	0.30±0.17	0.00±0.08	0.01±0.12
$T_i(a/2)$	-0.36±0.09	0.77±0.12	-0.28±0.13	0.18±0.06	0.33±0.07
$E_i/T_i(a/2)$	0.92±0.15	0.16±0.19	0.56±0.18	-0.02±0.08	-0.38±0.11
IOC					
$T_e(a/2)$	-0.56±0.12				0.20±0.10
$E_e/T_e(a/2)$	1.11±0.26				-0.07±0.14
$T_i(a/2)$	-0.33±0.12				0.21±0.11
$E_i/T_i(a/2)$	1.47±0.40				-0.76±0.33

Table 1: Scaling laws of the temperatures in the three confinement regimes. The ratio $E/T(a/2)$ is almost equal to the line–averaged density $\overline{n_e}$ (electrons) or $\overline{n_i}$ (ions). In the LOC regime the principal component Z^*_{eff} as defined in Eq. (2) is used.

of E_e on the toroidal field is slightly influenced by profile effects due to sawteeth.

The ion energy is similarly treated. The resulting scaling laws are

$$\begin{aligned} E_i^{LOC} &= 9.4kJ \times \overline{n_e}^{1.46\pm0.07} I_p{}^{0.57\pm0.18} B_t{}^{0.00\pm0.15} \\ &\times A_i{}^{0.10\pm0.05} Z^*_{eff}{}^{-0.30\pm0.10}, \qquad (15) \\ E_i^{SOC} &= 14.0kJ \times \overline{n_e}^{0.56\pm0.12} I_p{}^{0.93\pm0.15} B_t{}^{0.28\pm0.12} \\ &\times A_i{}^{0.16\pm0.06} Z_{eff}{}^{-0.05\pm0.09}, \qquad (16) \\ E_i^{IOC} &= 5.1kJ \times \overline{n_e}^{1.14\pm0.39} Z_{eff}{}^{-0.55\pm0.31}. \qquad (17) \end{aligned}$$

To treat the ion energy in the same way as the electron energy, it is compared with $\overline{n_i}T_i(a/2)$. It must be taken into account that $\overline{n_i} \sim \overline{n_e}^{1.3}$ in LOC, $\overline{n_i} \sim \overline{n_e}$ in SOC and $\overline{n_i} \sim \overline{n_e}^{1.4}$ in IOC. The density scaling of E_i in LOC is completely caused by this behaviour of $\overline{n_i}$, because there the ion temperature has only a small influence. In both of the other regimes $T_i(a/2)$ contributes to the density dependence with an exponent around -0.35 (see Tab. 1). The exponents of I_p and Z_{eff} in Eqs. (15–17) are almost identical to the exponents caused by $\overline{n_i}T_i(a/2)$. In contrast to this, the small isotope effect of the ion energy originate only from $T_i(a/2)$. Similarly to the properties of the electron energy, variations of B_t change the shapes of the profiles of the density and the temperature, giving an exponent for B_t in the energy scaling which cannot be explained only by the features of an averaged temperature $T_i(a/2)$. Apart from this, the ion energy is well described by $E_i \sim \overline{n_i}T_i(a/2)$ in all three confinement regimes.

The most impressive result, however, is the isotope effect of the ion energy, which is clearly weaker than that of the electron energy. Within the error bars of the exponents of A_i in both the LOC and SOC regimes the ion energy scales as less than $A_i^{1/6}$. Hence, the behaviour of the ions cannot explain the isotope effect of τ_E in ohmic ASDEX discharges.

5 Reconstruction of τ_E

Combination of the individual confinement laws gives new expressions for τ_E where the electron and the ion components are separated as shown in the following equation. A comparison of this expression with the explicit scaling laws of τ_E directly shows the influence of the electrons and the ions on τ_E:

$$\tau_E = \frac{2E_e}{P_{OH}} \times \frac{1}{2}\left(1 + \frac{E_i}{E_e}\right) , \tag{18}$$

where $2E_e/P_{OH}$ can be seen as the confinement time of an equilibrated plasma with equal densities and temperatures of the ions and electrons. The influence of the ion energy is now restricted to the second part of this definition, especially to the ratio of the ion and electron energies.

The resulting expressions are

$$\begin{aligned} \widetilde{\tau_E^{LOC}} &\sim \overline{n_e}^{0.61} I_p^{-0.57} B_t^{0.37} A_i^{0.49} Z_{eff}^{*\,-0.12} \\ &\times \left(1 + 0.89\overline{n_e}^{0.85} I_p^{-0.32} B_t^{-0.20} A_i^{-0.23} Z_{eff}^{*\,-0.49}\right) , \end{aligned} \tag{19}$$

$$\begin{aligned} \widetilde{\tau_E^{SOC}} &\sim \overline{n_e}^{0.17} I_p^{-0.29} B_t^{0.19} A_i^{0.43} Z_{eff}^{0.38} \\ &\times \left(1 + 0.69\overline{n_e}^{0.06} I_p^{0.07} B_t^{0.50} A_i^{-0.10} Z_{eff}^{-0.47}\right) , \end{aligned} \tag{20}$$

$$\widetilde{\tau_E^{IOC}} \sim \overline{n_e}^{0.55} Z_{eff}^{-0.11} \left(1 + 0.62\overline{n_e}^{0.59} Z_{eff}^{-0.68}\right) . \tag{21}$$

A comparison of these approximations (Eqs. (19–21)) with the original scaling laws for τ_E (Eqs. (3–5)) shows that τ_E mainly depends on E_e/P_{OH}.

For the LOC regime an exponent of 0.61 at the density in Eq. (19) is reached by using the electron energy only. Here the ohmic power does not depend on the density. Almost identical exponents are reached for the current, the magnetic field and the mass number by the direct scaling of τ_E and the scaling of E_e/P_{OH}. Especially the isotope effect of τ_E is caused by the behaviour of E_e and P_{OH} only, reflecting the fact that the magnitude of the electron temperature is strongly dependent on the mass number.

The influence of the ion energy in the LOC regime is restricted to small variations of the exponents of $\overline{n_e}$ and Z_{eff}^*. This can be seen from the second part of Eq. (19) describing the ratio of E_i and E_e. There, only the exponents of $\overline{n_e}$ (0.85) and Z_{eff}^* (-0.49) are high enough to alter the exponents formed by E_e/P_{OH}. This is caused by the strong variation of the ion density with increasing plasma density. It lets the ion energy increase faster than the electron energy. This leads to a small rise of the density exponent from 0.61 of

Eq. (19) to 0.86 of the direct scaling law for τ_E. For the same reason the exponent at Z^*_{eff} is lowered from -0.12 to -0.30. These, however, are only marginal changes.

Similar results are found for the SOC regime. The original scaling law (Eq. (4)) is nearly identical to E_e/P_{OH} from Eq. (20). Here only a slight variation with $\overline{n_e}$ can be found. This is caused by the density dependence of P_{OH}, which scales as $\overline{n_e}^{0.31}$. Thus the natural increase of the electron energy with the density is diminished to the resulting exponent 0.17 of τ_E. Considering only scaling law (20), however, does not allow any clear statement except that the influence of Z_{eff} on τ_E is definitely caused by the ion behaviour. A more stringent result is obtained for the isotope effect in the SOC regime: Discussion of the global scalings already shows that it cannot be explained at all by the use of the ion energy or the ion energy transport behaviour only. It enters the τ_E scaling via the electron energy and P_{OH}. For the other parameters, so far a scaling of E_i/P_{OH} instead of E_e/P_{OH} — which would perhaps indicate a dominant transport channel if the two scalings were significantly different — yields a similar result because the temperatures of the two species are nearly identical and the effective charge is independent of other global parameters.

As seen in the former section, the ion energy transport is responsible for the transport of at most only one–third of the total ohmic power. Hence, the energy confinement time in this regime is more influenced by the features of the electron energy transport. Apart from the fact that E_e/P_{OH} already reflects the dependences of τ_E (except that on Z_{eff}), the physical reason for the behaviour of τ_E in this regime is found to be caused more by the electron energy transport than by the ion energy transport.

This result is close to the findings in [6], where the local energy transport of both species is discussed by means of simulation calculations.

The situation for the IOC regime (Eqs. (5, 21)) is similar to that for the LOC regime. The density dependence of τ_E is explained by the behaviour of the electron energy only. The ohmic power does not affect the scaling. Even the behaviour of the ion energy influences the exponent of the density only marginally. The negative exponent of τ_E at Z_{eff} originates completely from variations of the ion energy .

From a statistical point of view, the IOC regime is a direct continuation of the LOC regime, where the energy transport mechanisms — especially the electron heat conduction — which cause the saturation in the SOC regime are suppressed. The common aspects of this improved regime allow the assumption that it is the ohmic counterpart to the "Z–mode" which was found in the ISX–B tokamak [30].

6 Conclusions

By means of statistics it is shown that in all three ohmic confinement regimes in ASDEX the energy confinement time τ_E is well described by the properties of the electron energy and the ohmic power only. Amongst other features of τ_E, the two most popular effects, viz. the density scaling, which is almost linear in LOC and IOC and saturates in SOC, and the isotope effect with $\tau_E \sim \sqrt{A_i}$, are attributed to the dependences of E_e and P_{OH}, while the ion energy does not significantly contribute. Hence, a further conclusion is that the ohmic confinement is mainly caused by the electron heat conduction. There is no evidence that the ion energy transport is responsible for the general aspects of the ohmic confinement time in ASDEX.

Furthermore, it is concluded that — with respect to the electrons — the improved IOC regime is a continuation of the low–density linear LOC regime. It is presumed that in the IOC regime the electron energy transport mechanisms causing the saturation in SOC are suppressed.

References

[1] PARKER, R. R., GREENWALD, M., LUCKHARDT, S. C., MARMAR, E. S., PORKOLAB, M. and WOLFE, S. M., Nucl. Fusion **25** (1985) 1127.

[2] GRUBER, O., Nucl. Fusion **22** (1982) 1349.

[3] BARTLETT, D. V. et al., Nucl. Fusion **28** (1988) 73.

[4] ALLADIO, F. et al., in Plasma Physics and Controlled Nuclear Fusion Research (Proc. 13th Int. Conf. Washington, 1990), Vol. 1, IAEA, Vienna (1991) 153.

[5] SÖLDNER, F. X. et al., Phys. Rev. Lett. **61** (1988) 1105.

[6] BECKER, G., Nucl. Fusion **30** (1990) 2285.

[7] DOMINGUEZ, R. R. and WALTZ, R. E., Nucl. Fusion **27** (1987) 65.

[8] MURAKAMI, M. et al., Phys. Rev. Lett. **42** (1979) 655.

[9] ROMANELLI, F., TANG, W. M. and WHITE, R. B., Nucl. Fusion **26** (1986) 1515.

[10] LEE, G. S. and DIAMOND, P. H., Phys. Fluids **29** (1986) 3291.

[11] GRUBER, O., in Plasma Physics (Proc. Int. Conf. Lausanne, 1984), Part 1, Commission of the European Communities, Brussels (1984) 67.

[12] FUSSMANN, G. et al., in Plasma Physics and Controlled Nuclear Fusion Research (Proc. 12th Int. Conf. Nice, 1988), Vol. 1, IAEA, Vienna (1989) 145.

[13] RÖHR, H., STEUER, K.-H., MURMANN, H. and MEISEL, D., Internal Report IPP III/121, Max–Planck–Institut für Plasmaphysik, Garching (1987).

[14] AFROSIMOV, V. V. and KISLYAKOV, A. I., in Proc. of the Course Diagnostics for Fusion Reactor Conditions, Varenna (1982) 289.

[15] FAHRBACH, H. U., HERRMANN, W. and MAYER, H. M., in Controlled Fusion and Plasma Physics (Proc. 16th Eur. Conf. Venice, 1989), Vol. 13B, Part IV, European Physical Society, Geneva (1989) 1537.

[16] RÖHR, H. and STEUER, K.-H., Rev. Sci. Instrum. **59** (1988) 1875.

[17] STEUER, K.-H. et al., in Controlled Fusion and Plasma Physics (Proc. 17th Eur. Conf. Amsterdam, 1990), Vol. 14B, Part I, European Physical Society, Geneva (1990) 62.

[18] SCHNEIDER, U. et al., J. Nucl. Mater. **176 & 177** (1990) 350.

[19] SIMMET, E. E., Internal Report IPP III/198, Max–Planck–Institut für Plasmaphysik, Garching (1994).

[20] GARBET, X. et al., Nucl. Fusion **32** (1992) 2147.

[21] WAGNER, F. et al., in Controlled Fusion and Plasma Physics (Proc. 16th Eur. Conf. Venice, 1989), Vol. 13B, Part I, European Physical Society, Geneva (1989) 195.

[22] BESSENRODT-WEBERPALS, M. et al., Nucl. Fusion **33** (1993) 1205.

[23] BRAVENEC, R. V. et al., Plasma Phys. Controlled Fusion **27** (1985) 1335.

[24] EJIMA, S. et al., Nucl. Fusion **22** (1982) 1627.

[25] EFTHIMION, P. C. et al., in Plasma Physics and Controlled Nuclear Fusion Research (Proc. 10th Int. Conf. London, 1984), Vol. 1, IAEA, Vienna (1985) 29.

[26] WAGNER, F., BESSENRODT-WEBERPALS, M., KALLENBACH, A., MCCORMICK, K., SÖLDNER, F. X. and STROTH, U., in Controlled Fusion and Plasma Physics (Proc. 17th Eur. Conf. Amsterdam, 1990), Vol. 14B, Part I, European Physical Society, Geneva (1990) 58.

[27] POSCHENRIEDER, W. et al., in Controlled Fusion and Plasma Physics (Proc. 13th Eur. Conf. Schliersee, 1986), Vol. 10C, Part I, European Physical Society, Geneva (1986) 196.

[28] HINTON, F. L. and HAZELTINE, R. D., Rev. Mod. Phys. **48** (1976) 239.

[29] BARTIROMO, R., in Controlled Fusion and Plasma Physics (Proc. 18th Eur. Conf. Berlin, 1991), Vol. 15C, Part I, European Physical Society, Geneva (1991) 73.

[30] LAZARUS, E. A. et al., J. Nucl. Mater. **121** (1984) 61.